



## Efficient amine-SBA-15-type adsorbents for treatment of water containing trace levels of Pb(II) and Cd(II)

Victoria Gascón<sup>a</sup>, Amaya Arencibia<sup>b,\*</sup>, Jesús María Arsuaga<sup>b</sup>

<sup>a</sup>Department of Chemical Sciences, Bernal Institute, University of Limerick, Limerick, V94T9PX, Ireland,  
email: Victoria.GasconPerez@ul.ie

<sup>b</sup>Chemical and Environmental Engineering Group, Department of Energy, Mechanical and Chemical Technology,  
ESCET – Universidad Rey Juan Carlos, C/Tulipán s/n, Móstoles (Madrid) Spain, Tel. +34 91 488 70 85; Fax: +34 91 488 70 68;  
emails: amaya.arencibia@urjc.es (A. Arencibia), jesusmaria.arsuaga@urjc.es (J.M. Arsuaga)

Received 10 July 2018; Accepted 9 December 2018

### ABSTRACT

Multiamine materials were prepared from SBA-15 mesoporous silica by grafting and impregnation methods. Polyethylenimine and two organosilanes containing amino groups: [amino-ethylamino]-propyltrimethoxysilane (NN), [(2-aminoethylamino)ethylamino]propyl-trimethoxysilane (NNN) were used as supply of the organic chains. These functionalized materials were used as adsorbents for the removal of aqueous lead(II) and cadmium(II), which are included in the EU list of Priority Substances in Water. The prepared materials were characterized by XRD, nitrogen adsorption-desorption, <sup>29</sup>Si MAS NMR, and elemental analysis. Experimental adsorption isotherms were determined up to saturation and successfully reproduced with the Langmuir model. The influence on Pb(II) and Cd(II) adsorption of the type of functional organic chain incorporated and the percentage of functionalization was studied. Likewise, pH effect and sorption mechanism were analyzed. Consequently, maximum adsorption capacities were significantly superior for Pb(II) achieving values as high as 1.37 mmol Pb g<sup>-1</sup>. Furthermore, the observed strong affinity between adsorbent and metals at trace-level concentrations evidenced potential industrial application of these adsorbents for Pb(II) and Cd(II) uptake in contaminated water treatments.

*Keywords:* Amine-functionalized SBA-15; Water treatment; Selective adsorption; Lead and cadmium removal

### 1. Introduction

World Health Organization (WHO) recent studies show how billions of people globally are presently drinking tap water contaminated by heavy metals at a trace level [1,2]. Among them, lead and cadmium are hazardous pollutants commonly found in aquatic effluents as they are discharged from several industries [3–5]. As heavy metals, they cannot be destroyed and thus, they can be accumulated throughout the food chain, being noxious for both living organisms in water media and for humans. Their high toxicity, even at a very low concentration, has made international legislation to establish restrictive limits for their concentration levels in water [6].

Cadmium metal and its compounds are defined as priority hazardous substances in the field of water policy since 2011 (2000/60/EC Directive according to the 2455/2001/EC resolution) which led the maximum allowable concentration for environmental quality standards (MAC-EQS) to be lower than 1.5 µg L<sup>-1</sup> [7]. Furthermore, according to 2013/39/EU Directive, EQS values for cadmium and its compounds vary depending on the water hardness [8]. In the case of lead, the value for MAC-EQS is also regulated and its proposed limit has been recently reduced to 14 µg L<sup>-1</sup> [8,9]. The values recommended by WHO for drinking water are 10 and 3 µg L<sup>-1</sup> for Pb(II) and Cd(II), respectively [1], and similar limits are worldwide prescribed [2].

\* Corresponding author.

To remove toxic heavy metals from wastewater, remediation methods including chemical precipitation and adsorption are usually effective. The adsorption technique is popular due to its easy operation, low-energy consumption, simple maintenance, and its large capacity [10,11]. However, although the common adsorbents including activated carbons have been used for metals removal, they are indeed nonselective and, besides, they are not recommended for reducing aqueous concentration below the legally required ppb limits [12].

Among selective adsorbents, those based on mesostructured silica materials are being widely investigated with the aim of developing a standard technology for treating wastewater containing heavy metals at very low concentrations. Mesoporous silica materials which are chemically functionalized with organic groups exhibit remarkable ability as adsorbents in water remediation applications. They show excellent textural properties to be used as bespoke adsorbents, showing high surface areas, high pore volumes and homogeneous pore diameters. Furthermore, the organic groups anchored to the silica walls promote specific affinity towards target metallic species [13]. Apart from the extensive work focused on mercury removal by silica functionalized with organic sulphur [13–15], some other studies have been carried out in relation with the synthesis of amine-modified adsorbents with the intention of eliminating metals in water including copper, zinc, nickel, or cobalt [13,16]; nevertheless, deeper studies cannot be commonly found relative to the specific removal of hazardous cadmium and lead species.

Some investigations have been conducted by incorporating complex organic ligands such as highly branched poly-amidoamine dendrimers (PAMAM) [17,18], humic acids that contains carboxylic and phenolic groups [19], or guanidine organic entities [20], but in none of those the reported maximum adsorption capacities were significantly high. Nevertheless, more successful results were reported regarding the study of SBA-15 functionalized with melamine-based dendrimer amines employed for the adsorption of Pb(II), Cd(II), and Cu(II), having maximum capacities of 0.62 mmol g<sup>-1</sup> and 0.87 mmol g<sup>-1</sup> for lead and cadmium, respectively [21].

Lead removal has also been tested by ion-imprinted polymer derived from chitosan supported on SBA-15 [22] obtaining 0.2 mmol Pb g<sup>-1</sup>, or other materials based on molecular recognition with a di(aminocyclohexyl)-18 crown-6 with high metal recovery at 100 ppm [23]. Formerly, the functionalization of mesostructured silica with EDTA was reported to be suitable for removing Pb(II) [24], and other metals [25], being possible to achieve an adsorption capacity of 1.1 mmol Cd(II) g<sup>-1</sup> and 1.32 mmol Pb(II) g<sup>-1</sup> through a complex process involving ion exchange and surface complexation. For the specific adsorption of cadmium, the incorporation of iminodiacetic acid in SBA-15 has been tested with an adsorption capacity of 0.25 mmol Cd(II) g<sup>-1</sup> [26].

However, the above-mentioned materials usually require the synthesis of complex organic molecules by several synthesis steps before or after grafting the silica mesostructured surface. More simplex organic compounds based on alkylamines have been reported to achieve good results. Benhamou et al. [27] and Sayari et al. [28] studied the adsorption of Pb(II), Cd(II), and other metals by pore expanded MCM-41 and MCM-48 materials obtained through the post-synthesis pore expansion procedure developed by Sayari's group.

Alternatively, aminopropyl (AP), ethylenediamine (ED), and diethylenetriamine (DT) were proposed to develop efficient adsorbents for aqueous lead and cadmium, along with copper, cobalt, or iron [29–31]. AP was widely studied [16,32–35], particularly for copper [34,36–39]. It has been reported that the adsorption was higher for lead(II) than for cadmium(II) [40,41]. In addition, the mechanism of interaction between Pb<sup>2+</sup> ions and R-NH<sub>2</sub> groups located on the adsorbent surface has been investigated by Hernandez-Morales et al. [42].

Conversely, few studies have been reported regarding multiamine functionalized materials for heavy metal removal. Faghihian and Naghavi [43] compared the adsorption properties of mesoporous silica MCM-41 and MCM-48 functionalized with ethylenediamine for Pb(II) and Cd(II), among other metals. Machida et al. [44] studied the role of diverse functional groups (mono, di, triamine, thiol, or carboxylic groups) on MSU and hexagonal mesoporous silica (HMS) as adsorbents of cadmium [44], while Xia et al. [45] investigated the adsorption properties of several mesostructured silicas at low concentration of Pb, Cd, Fe, Mn, and As. Our group reported an extensive work focused on the preparation of amine-functionalized SBA-15 with one (N, AP), two (NN, ED), or three (NNN, DT) amino groups [46]. In that study, preliminary tests were carried out for the adsorption of Cu(II), Pb(II), Cd(II), and other metals. Cu(II) removal was studied in detail with adsorption capacities very enhanced when using organic precursors containing several amino groups per molecule.

Therefore, as the SBA-15 mesostructure is very stable and offers excellent porous properties due to its open pore structure, our aim in this work is to obtain materials with a high amount of amino groups using multiamine as precursor in order to develop efficient adsorbents for aqueous lead and cadmium [47,48]. We present a detailed study on the synthesis and characterization of multiamine-prepared mesostructured SBA-15 materials that were mostly obtained by grafting the surface with ethylenediamine (ED) and DT. The influence of the amount and type of organosilane groups employed, together with the influence that has got the surfactant removal method on the physicochemical properties of adsorbents and the equilibrium adsorption of lead and cadmium is discussed. Furthermore, the preparation of materials obtained by polyethylenimine (PEI) impregnation [47,48] has been accomplished and their adsorption capacity was evaluated for cadmium. Besides, the ability of all of these materials to reduce the heavy metal concentration below the limits allowed by the international legislation on drinking water has been examined.

## 2. Experimental section

### 2.1. Chemical reagents

All the chemicals used for synthesis were supplied by Sigma-Aldrich. Tetraethyl orthosilicate (TEOS) and triblock copolymer poly(ethylene oxide)-poly(propylene oxide)-poly(ethylene oxide) Pluronic P123 (MW = 5,800) were used as the silica source and structure directing agent, respectively, for SBA-15. The functionalization agents used for grafting were [amino-ethylamino]-propyltrimethoxysilane (NN) and [(2-aminoethylamino)ethylamino] propyltrimethoxysilane (NNN). PEI was used for the impregnation of SBA-15 silica surface (branched PEI, average molecular weight 800,  $\rho = 1.05 \text{ g mL}^{-1}$ ).

Sources of metals for adsorption experiments were cadmium nitrate and lead nitrate that are reagent grade and were supplied from Scharlab (Spain). Lead(II) atomic spectroscopy standard  $1.0 \text{ g L}^{-1}$  and cadmium(II) atomic spectroscopy standard  $1.0 \text{ g L}^{-1}$  were supplied by Fluka (Sigma-Aldrich, Spain). Hydrochloric acid, nitric acid, methanol, ethanol, and toluene were provided from Scharlab. Solvents were all analytical or HPLC grade. All materials were used as received, without further purification. Water purity was Milli-Q grade.

## 2.2. Adsorbents synthesis

Pure silica SBA-15 was synthesized by using Pluronic P123 triblock copolymer according to the bibliography [49,50]. The white solid product was recovered by filtration, washed with ethanol and air dried. The organic template was removed by using two different procedures: calcination (C) at  $550^\circ\text{C}$  or extraction (E) by ethanol reflux. The obtained mesoporous materials, denoted as SBA-15-C and SBA-15-E, were functionalized with two different amino chains [amino-ethylamino]-propyl (denoted as ED or NN) and [(2-aminoethylamino)ethylamino]propyl (denoted as DT or NNN). The grafting was accomplished through the silanization reaction of the surface silanol groups with the aminosilane precursors. The molar degree of functionalization (X%) in the grafting mixture was varied between 15% and 40%. The resulting functionalized materials were designated as SBA-15-E-NN-X%, SBA-15-E-NNN-X%, SBA-15-C-NN-X%, and SBA-15-C-NNN-X%, respectively.

In addition, pure calcined SBA-15 (SBA-15-C) was impregnated with an organic polymer, PEI, according to Sanz et al. [51]. The impregnation was carried out by adding different amounts of the PEI polymer to obtain 30% and 50% weight of organic component in the final product. These adsorbents were denoted as SBA-15-C-PEI-X%, where now X represents the weight percentage of PEI in the final solid.

## 2.3. Characterization

Mesoscopic order was investigated by low-angle X-ray diffraction (XRD). Patterns of the samples were obtained on a powder PW3040/00 X'Pert MPD/MRD diffractometer using Cu K $\alpha$  radiation. Nitrogen adsorption–desorption isotherms were measured at 77 K using Micromeritics Tristar 3000 sorptometer. Prior to the measurements, samples were outgassed under nitrogen during 8 h at  $200^\circ\text{C}$  and  $150^\circ\text{C}$  for pure silicas and functionalized adsorbents, respectively. The specific surface area,  $S_{\text{BET}}$  was calculated from nitrogen adsorption data in the relative pressure range from 0.04 to 0.2 using the Brunauer–Emmet–Teller (BET) method [52]. The total pore volume,  $V_{\text{ads}}$  was determined from the amount of nitrogen adsorbed at a relative pressure  $P/P_0$  of 0.97 [52]. Pore size distributions were obtained from the adsorption branch of the nitrogen isotherms using the Barrett–Joyner–Halenda model assuming a cylindrical geometry of the pores. Structural parameters of the synthesized mesoporous materials, such as the unit cell parameter ( $a_0$ ) and the wall thickness ( $e_p$ ), were obtained by combining XRD and nitrogen sorption data.

Nitrogen content of amine-functionalized adsorbents was determined by elemental analysis, on a CHNOS

model Vario EL III of Elemental Analyses System, GmBh (Germany). The amine loading was calculated from the nitrogen content.

Solid state  $^{29}\text{Si}$  MAS NMR spectra were collected on a Varian Infinity 400 instrument operating at 79.4 MHz. Tetramethylsilane was used as a reference for establishing the chemical shifts. Runs were carried out under magic-angle spinning at 6.0 kHz with 90 pulses of 4.51 s and delay time of 15 s.

## 2.4. Heavy metal adsorption experiments

Adsorption of lead, Pb(II), and cadmium, Cd(II), on functionalized materials was investigated through batch equilibrium experiments. The adsorbent-solution mixtures consisted of 45 mL of heavy metal aqueous solution (concentration range  $5\text{--}300 \text{ mg L}^{-1}$ ) and 25 mg of adsorbent at  $25^\circ\text{C}$  controlled temperature. Equilibrium time has been reported for the adsorption of different inorganic species on functionalized mesostructured adsorbents to vary between 30 and 120 min depending on contaminant concentration [46,53,54]. For these experiments, suspensions were magnetically stirred for 180 min, time much longer than the previously established to reach equilibrium for any concentration value [46]. Then, the solution was filtered with a syringe filter ( $0.22 \mu\text{m}$  pore size) and the residual heavy metal solution was collected. Metal concentration in all aqueous solution was analysed by inductivity coupled plasma atomic emission spectroscopy. Measurements were performed in a Varian Vista AX spectrometer after calibration with stock solutions in the concentration range  $0\text{--}10 \text{ mg L}^{-1}$ .

The amount of heavy metal adsorbed at equilibrium,  $q_e$  ( $\text{mmol g}^{-1}$ ), was determined by difference between initial and equilibrium metal concentration in the solutions as follows:

$$q_e = (C_o - C_e) \cdot \frac{V}{m \cdot M} \quad (1)$$

where  $q_e$  is the adsorbed amount at equilibrium ( $\text{mmol g}^{-1}$ ),  $V$  is the total volume of Cd(II) or Pb(II) solution used in every adsorption experiment (45 mL),  $m$  is the mass of adsorbent (25 mg),  $C_o$  is the initial concentration of Cd(II) or Pb(II) solutions ( $\text{mg L}^{-1}$ ),  $C_e$  is the equilibrium Cd(II) and Pb(II) concentration ( $\text{mg L}^{-1}$ ), and  $M$  is the molar mass of the heavy metal studied, lead or cadmium. Percentage removal,  $R$  (%), was calculated according to Eq. (2):

$$R(\%) = \frac{C_o - C_e}{C_o} \cdot 100 \quad (2)$$

## 3. Results and discussion

### 3.1. Characterization of SBA-15 adsorbents

#### 3.1.1. Amine-functionalized silica SBA-15

Mesoporous silica adsorbents functionalization with organic chains containing multiple amino groups, denoted as NN and NNN, was carried out by grafting the surface of pure SBA-15 prepared through two alternative surfactant removal procedures, calcination and extraction. Fig. S1 shows the

low-angle XRD patterns of calcined and extracted SBA-15 materials (SBA-15-C and SBA-15-E, respectively) compared with several functionalized materials, SBA-15-C/E-NN-X% and SBA-15-C/E-NNN-X%. Three diffraction peaks corresponding to (1 0 0), (1 1 0), and (2 0 0) family planes were detected for each pure silica sample, which can be indexed to a two-dimensional hexagonal lattice characteristic of the mesoporous material SBA-15 [50]. The relative intensity of the reflections diminished for functionalized samples due to the increased organic content inside the pores. Diffractograms corresponding to adsorbents containing diamine organic chains, SBA-15-C/E-NN, still exhibit the well-resolved reflections corresponding to (1 1 0) and (2 0 0) for both types of silica so indicating that the mesoporous structure was preserved after the incorporation of amino groups, although lower intensities were thoroughly found for structures obtained by extraction procedure (SBA-15-E-NN). However, materials obtained by grafting the silica surface with diethylenetriamine chains, SBA-15-C/E-NNN, yield diffractograms with significant reduction of (1 1 0) and (2 0 0) reflexions; hence, one single distinctive diffraction peak was found for almost all these triamine-modified materials.

Fig. S2 shows some representative  $N_2$  adsorption-desorption isotherms measured at 77 K, along with the calculated pore size distributions (inset), for pure silica SBA-15-C/E and functionalized samples (SBA-15-C/E-NN-X% and SBA-15-C/E-NNN-X%). As observed, all the functionalized materials maintained the characteristic type IV isotherm and uniform pore sizes within the mesoporous range. Therefore, it can be concluded that the SBA-15 structure was successfully preserved after functionalization.

Textural parameters estimated from  $N_2$  adsorption-desorption isotherms are summarized in Table 1. As expected, an evident decrease of those parameters is systematically observed for amine-functionalized materials. Thus, the parameters corresponding to calcined samples (SBA-15-C) grafted with diamine (NN) gradually decrease from 83 to 59 Å ( $D_p$ ), 604 to 156  $m^2 g^{-1}$  ( $S_{BET}$ ), and 0.95 to 0.27  $cm^3 g^{-1}$  ( $V_p$ ) as the functionalization percentage raises from pure silica to SBA-15-C-NN-30%. For diethylenetriamine (NNN) materials,

a reduction of around 30%, 60%, and 45% is observed for  $D_p$ ,  $S_{BET}$  and  $V_p$ , respectively, higher than that corresponding to diamine modified solids and almost independent from the functionalization percentage.

The textural properties decline of adsorbents prepared from extracted silica (SBA-15-E) is rather similar to that obtained for calcined samples with a slight difference: the length of the amine chains hardly affects the parameters. For example, the pore size remains close to 81 Å for the functionalized SBA-15-E-NN/NNN materials.

Regarding the structural information displayed in Table 1, a slight reduction in the unit cell parameter  $a_0$  of calcined samples was found as compared with the pure silica parent structure, whereas for extracted materials no clear changes were evidenced. Besides, the wall thickness ( $e_p$ ) was systematically enlarged due to amine functionalization; however, no evident correlation was found between the extent of organic chains incorporation and wall thickness.

The analysis of nitrogen content and the calculated molar amount of organic chain in calcined samples revealed that when functionalizing agent percentage in the grafting mixture was raised from 15% to 30%, an insignificant increase of incorporated nitrogen was detected both for SBA-15-C-NN (3.15 and 3.21  $mmol N g^{-1}$ ) and SBA-15-C-NNN (3.92 and 3.98  $mmol N g^{-1}$ ). Conversely, the increment was apparent for SBA-15-C-NNN-40%. The grafting process was more efficient for extracted materials than for calcined ones, showing an enhanced organic functionalization probably due to the increased availability of silanol groups on their surface [55]. The maximum nitrogen content attained by grafting in this study was 4.82  $mmol g^{-1}$  (SBA-15-C-NNN-40% and SBA-15-E-NNN-15%).

For each SBA-15 precursor, calcined or extracted, the nitrogen content of the final material increased when the number of amino groups per organosilane molecule was higher (NNN > NN). However, the molar amount of organic chains incorporated into the adsorbents was always smaller for samples functionalized with diethylenetriamine (NNN). For example, SBA-15-C-NN-15% material contains 1.57  $mmol g^{-1}$  against 1.31  $mmol g^{-1}$  corresponding to SBA-15-C-NNN-15%.

Table 1

Textural and structural properties of sorbents synthesized from calcined (C) and extracted (E) SBA-15 by grafting of organic polyamine chains (NN and NNN) and polyethylenimine impregnation (PEI). Nitrogen content obtained from CHNSO elemental analysis is also displayed

Material	Textural properties			Structural properties			Nitrogen content	
	$D_p$ (Å)	$S_{BET}$ ( $m^2 g^{-1}$ )	$V_p$ ( $cm^3 g^{-1}$ )	$d_{100}$ (Å)	$a_0$ (Å)	$e_p$ (Å)	N ( $mmol g^{-1}$ )	Org. Chain ( $mmol g^{-1}$ )
SBA-15-C	83	604	0.95	101	117	34	–	–
SBA-15-C-NN-15%	71	284	0.49	97	112	41	3.15	1.57
SBA-15-C-NN-30%	59	156	0.27	99	114	56	3.21	1.60
SBA-15-C-NNN-15%	58	235	0.44	97	112	54	3.92	1.31
SBA-15-C-NNN-30%	57	262	0.44	97	112	55	3.98	1.33
SBA-15-C-NNN-40%	62	191	0.32	97	112	50	4.82	1.74
SBA-15-E	91	576	1.03	109	126	35	–	–
SBA-15-E-NN-15%	82	233	0.57	109	126	44	3.55	1.77
SBA-15-E-NNN-15%	80	240	0.51	112	129	49	4.82	1.61
SBA-15-C-PEI-30%	58	153	0.27	104	120	62	5.86	N/A
SBA-15-C-PEI-50%	59	49	0.09	104	120	61	9.64	N/A

This fact, previously observed for analogous materials, was attributed to restrictions in the diffusion of the NNN organosilane within the pores during the grafting reaction that resulted in limited accessibility toward the reactive surface silanol groups [46].

It is worth mentioning that the incorporation of higher amounts of functionalizing agent for extracted samples was tried with unsuccessful result when NN or NNN > 20% were used. For instance, the synthesis of SBA-15-NNN-40% yielded a material such as SBA-15-E-NN-20% [56].

Fig. 1 displays the  $^{29}\text{Si}$  MAS-NMR spectra of three amine-functionalized SBA-15 materials (SBA-15-C-NN-15%, SBA-15-C-NNN-15%, and SBA-15-E-NN-15%) selected to confirm the covalent incorporation of organosilanes to the silica walls. As visible in Fig. 1, the spectra profiles were split into individual Gaussian bands. Three pure silica characteristic peaks were assigned to  $Q^n$  [ $Q^n = \text{Si}(\text{OSi})_n(\text{OH})_{4-n}$ ,  $n = 2, 3, \text{ or } 4$ ],  $Q^4$  at  $\delta = -110$  ppm,  $Q^3$  at  $\delta = -100$  ppm, and  $Q^2$  at  $\delta = -90$  ppm. The two additional peaks appearing at higher chemical shift, namely  $T^m$  signals, [ $T^m = \text{R-Si}(\text{OSi})_m(\text{OH})_{3-m}$ ,  $m = 2 \text{ or } 3$ ],  $T^3$  at  $\delta = -65$  ppm, and  $T^2$  at  $\delta = -55$  ppm, indicated that the organic chains (R-) had been successfully grafted within the materials. The degree of organic incorporation was estimated through the signal intensity ratio,  $R_i = I(T^m)/I(Q^n)$  [57]. Measured ratios revealed that the incorporation was more effective for the extracted sample,  $R_i = 0.17$ , against  $R_i = 0.12$  found for each calcined material. These values were coherent with the corresponding organic chain content displayed in Table 1.

### 3.1.2. PEI impregnated silica samples

Impregnation of calcined SBA-15 silica with hyper-branched PEI was carried out for two PEI percentages (30% and 50%). Fig. S3(A) shows the low-angle XRD patterns as well as the characterization obtained from nitrogen adsorption-desorption isotherms at 77 K and pore diameter distributions

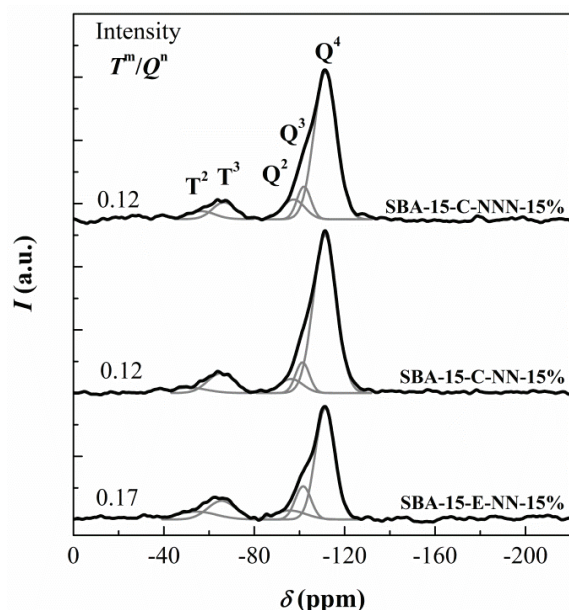


Fig. 1.  $^{29}\text{Si}$  MAS-NMR for selected amine-functionalized SBA-15 materials and relative peak intensities.

of the samples (Fig. S3(B)). Diffractograms confirmed the SBA-15 hexagonal structure for both impregnated silicas: SBA-15-C-PEI-30% and SBA-15-C-PEI-50%. The SBA-15-C-PEI-30% material exhibited the strong (1 0 0) reflection peak (at  $2\theta = 0.85^\circ$ ) and the smaller (1 1 0) and (2 0 0) diffraction signals, which are characteristic of a well-ordered SBA-15 type material. Conversely, SBA-15-C-PEI-50% showed a significant decrease in XRD peak intensities, providing evidence that impregnation occurred mainly inside the pore channels, as previously found [51].

Nitrogen sorption isotherms displayed the usual type IV profile for this type of SBA-15 material, hence confirming the characteristic nature of mesoporous materials. As observed, the incorporation of PEI on SBA-15 yields final structures with much reduced porosity compared with pure silica, especially for the SBA-15-C-PEI-50% sample barely shows capacity for  $\text{N}_2$  adsorption due to the filling of mesochannels. Concerning the values of textural parameters (Table 1), these materials exhibited a significant decrease of superficial area and pore volume when increasing PEI content, but maintained mesopore sizes around 58 Å. Thus, it can be concluded that the mesoporous structure was preserved after impregnation although the pores were almost completely filled with organic polymer.

As expected, samples obtained by PEI impregnation achieve much higher nitrogen content (5.86–9.64 mmol amine groups per gram of solid) than every material functionalized by grafting.

## 3.2. Heavy metal aqueous adsorption

The feasibility of amine-modified SBA-15 materials for the removal of lead and cadmium from aqueous solutions was evaluated by obtaining the whole equilibrium adsorption isotherms up to saturation at 25°C. Isotherms were constructed by aggregating multiple individual batch experiments using lead or cadmium nitrate as metal source. The materials selected for the adsorption study were SBA-15-C-NN-30%, SBA-15-C-NNN-30%, SBA-15-E-NN-15%, and SBA-15-E-NNN-15%. It has to be mentioned here that the adsorption capacity previously found for pure silica SBA-15 was negligible compared with amine-functionalized samples [46].

### 3.2.1. Lead adsorption isotherms

The experimental isotherms of Pb(II) adsorption from aqueous solution at 25°C are shown in Fig. 2 where the metal adsorbed amount at equilibrium ( $q_e$ ) is plotted vs. the equilibrium concentration in the liquid phase ( $C_e$ ). All the isotherms show characteristic type I shape in IUPAC classification [52] or type L according to the Giles classification [58], having a sharp initial slope, that indicates high efficiency of the adsorbent at low metal concentration, with a typical saturation constant value when aqueous Pb(II) concentration increases. The adsorption data were modelled using Langmuir and Freundlich equations in their linear forms [59,60]. As it is well-known, the Langmuir adsorption model (Eqs. (3) and (4)) was derived for surfaces with homogeneous adsorption sites having the same affinity that are covered by the adsorbate until filling the monolayer at high equilibrium concentration.  $Q_0$  and  $b$  are the maximum adsorbed amount in the monolayer

and the equilibrium constant of adsorption for Langmuir model. Freundlich isotherm (Eqs. (5) and (6)) should be considered for heterogeneous energetic surfaces, with  $k$  and  $n$  being empirical constants that are related to the uptake capacity of the adsorbent and the intensity of adsorption.

$$q_e = Q_o \cdot \frac{b \cdot C_e}{1 + b \cdot C_e} \tag{3}$$

$$\frac{C_e}{q_e} = \frac{1}{Q_o \cdot b} + \frac{1}{Q_o} \cdot C_e \tag{4}$$

$$q_e = k \cdot C_e^{1/n} \tag{5}$$

$$\log q_e = \log k + \frac{1}{n} \cdot \log C_e \tag{6}$$

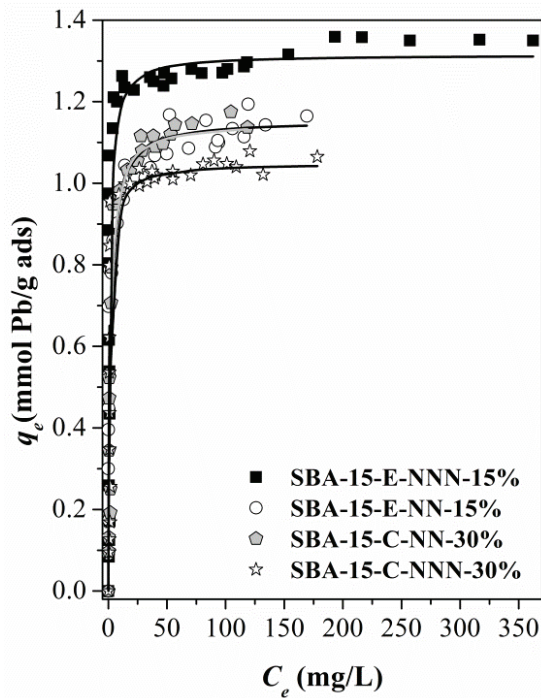


Fig. 2. Experimental Pb(II) adsorption isotherms at 25°C for extracted ‘E’ and calcined ‘C’ SBA-15 materials functionalized by grafting with NN and NNN organic chains.

Table 2  
Nitrogen content of materials, experimental maximum lead(II) capacity of adsorption, and fitting parameters of model isotherms

Material	N (mmol g <sup>-1</sup> )	Q <sub>o</sub> <sup>exp</sup> (mmol Cd g <sup>-1</sup> )	Langmuir isotherm			Ratio Q <sub>o</sub> /N	Freundlich isotherm		
			Q <sub>o</sub> (mmol Cd g <sup>-1</sup> )	b (L mg <sup>-1</sup> )	R <sup>2</sup>		k	n	R <sup>2</sup>
SBA-15-C-NN-30%	3.2	1.16	1.18	0.50	0.9988	0.36	0.35	3.14	0.84
SBA-15-C-NNN-30%	4.0	1.06	1.11	0.47	0.9989	0.27	0.39	4.23	0.70
SBA-15-E-NN-15%	3.6	1.15	1.15	0.53	0.9990	0.32	0.53	5.65	0.82
SBA-15-E-NNN-15%	4.8	1.37	1.36	0.60	0.9998	0.28	0.52	5.20	0.63

Note: Individual adsorption experiments: 45 mL of Pb(II) aqueous solution (C<sub>0</sub> = 5–300 mg L<sup>-1</sup>) and 25 mg of adsorbent. T = 25°C, natural pH.

Figs. S4(A) and (B) show the predictions of both models in their linear equation form. The obtained fitting parameters are presented in Table 2, along with the correlation coefficients. As seen, the values of R<sup>2</sup> for Langmuir are excellent (around 0.999), whereas those estimated from the Freundlich model are deficient (R<sup>2</sup> in the range 0.63–0.84), demonstrating the correctness of Langmuir model for reproducing the Pb(II) adsorption isotherm and confirming monolayer adsorption.

The comparison between adsorbents functionalized with different organosilanes yields dissimilar conclusions depending on the procedure used to remove the surfactant. From the extracted samples, it can be seen that material SBA-15-E-NNN-15% functionalized with DT (NNN) molecule exhibited maximum adsorption capacities higher than SBA-15-E-NN-15%, modified with ED (NN), reflecting that an increase in the nitrogen amount per molecule produces an increment of Pb(II) uptake. Conversely, the lower maximum adsorption capacity for calcined samples was found for SBA-15-C-NNN-30%, as compared with SBA-15-C-NN-30%, indicating that no improvement on the adsorption capacity of Pb(II) was attained. Here, the organosilane NNN chain incorporation is smaller, being this arguably due to the less probability of finding silanol groups for grafting in calcined SBA-15. Hence, although the nitrogen content is higher for NNN material, no improvement in the overall adsorption is achieved because the lower efficiency of nitrogen as lead binding in DT molecules comparatively with ED.

As it has been previously reported, adsorption capacity is not always proportional to the number of functional moieties incorporated to the material [29,31,61], indicating that the efficiency of amino groups can decrease with the loading amount [45]. Actually, Yokoi et al. [31] found that an increment of the AP and ED amounts yielded higher adsorption capacities, whereas this parameter did not always increase for DT. It must be taken into account that, for high density of multiamines, many active sites could be inactive due to porosity reduction or pore blockage. The latter factor can be originated by inhomogeneous grafting of functional groups located at the pore entrance irrespective of the silica pore diameter, avoiding the chemical interaction of heavy metal ions with the effective amino groups located inside the pores.

Moreover, the distribution of amino groups inside the pores could be more homogeneous in extracted samples, since functional groups could be better dispersed in presence of remaining surfactant being more difficult to find blocked pores and hence obtaining higher efficiency of amino groups [62–64]. Besides, the amount of organosilane

consumed during the synthesis from extracted silica is half the one needed to attain similar or poorer results with calcined SBA-15. Thus, it is concluded that extraction is the preferred procedure, being possible to obtain maximum Pb(II) adsorption capacities of  $1.37 \text{ mmol g}^{-1}$  ( $284 \text{ mg g}^{-1}$ ) with SBA-15-E-NNN-15%.

### 3.2.2. Cadmium adsorption isotherms

Fig. 3 displays the experimental isotherms for aqueous cadmium adsorption on amine-grafted SBA-15 materials. As for lead, all the isotherms exhibited a sharp initial slope, indicating that the grafted materials acted as high-efficiency adsorbents also at low metal concentration. When the initial aqueous cadmium concentration increased, saturation was easily attained. The equilibrium data were fitted using Langmuir and Freundlich models in their linear forms. Langmuir model (Fig. S5(A)) describes the adsorption better

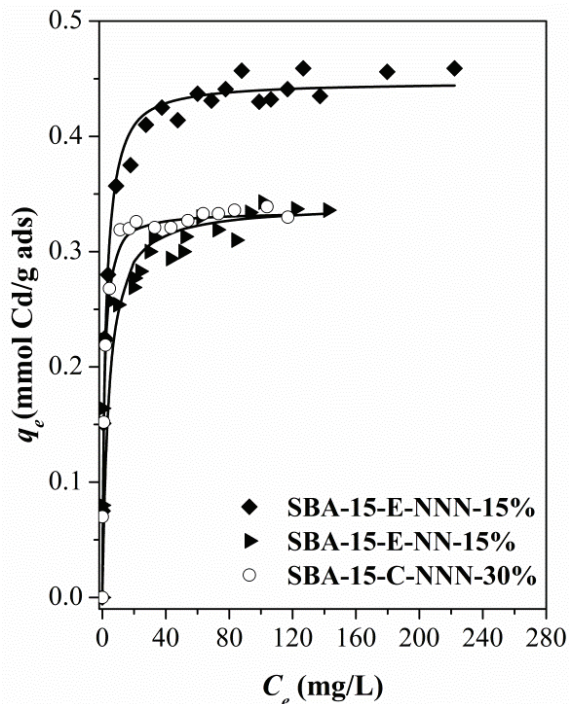


Fig. 3. Experimental cadmium adsorption isotherms at  $25^\circ\text{C}$  for extracted 'E' and calcined 'C' SBA-15 materials functionalized by grafting with NN and NNN.

than the Freundlich model (Fig. S5(B)), as confirmed by the fitting parameters shown in Table 3, where the experimental maximum adsorption capacities,  $Q_0^{\text{exp}}$ , along with the nitrogen content were also presented for each adsorbent. As seen, the maximum adsorption for calcined SBA-15-C-NNN-30% yields the same value ( $0.34 \text{ mmol Cd g}^{-1}$ ) than the extracted sample SBA-15-E-NN-15% that contains less nitrogen. For extracted materials, a significant increase on adsorption capacity was found when DT (NNN) was used instead of ED (NN) due to the increase of nitrogen content. Thus, the SBA-15-E-NNN-15% adsorbent showed the highest capacity for cadmium adsorption with a value of  $0.45 \text{ mmol g}^{-1}$  ( $50.6 \text{ mg Cd g}^{-1}$ ).

In the present study, PEI-impregnated SBA-15 was tested for aqueous cadmium removal to compare the performances of diverse adsorbents. Cd(II) adsorption isotherms shown in Fig. 4 can be classified as type I, but with profiles considerably different from the materials obtained by grafting due to two features: the smaller metal-adsorbent affinity at low concentration and the incomplete saturation at

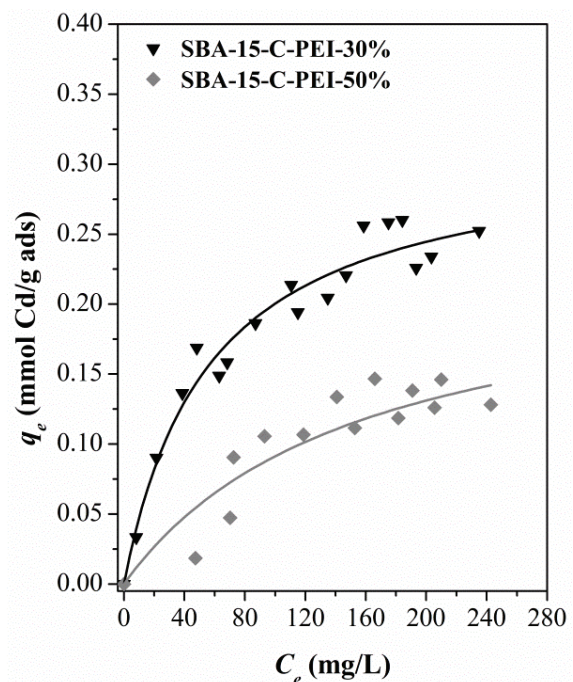


Fig. 4. Cd(II) adsorption isotherms at  $25^\circ\text{C}$  on calcined SBA-15 impregnated with PEI molecules.

Table 3

Nitrogen content of materials, experimental maximum cadmium(II) capacity of adsorption, and fitting parameters of model isotherms

Material	N (mmol $\text{g}^{-1}$ )	$Q_0^{\text{exp}}$ (mmol Cd $\text{g}^{-1}$ )	Langmuir isotherm			Ratio $Q_0/N$	Freundlich isotherm		
			$Q_0$ (mmol Cd/g)	$b$ (L/mg)	$R^2$		$k$	$n$	$R^2$
SBA-15-E-NN-15%	3.6	0.34	0.34	0.30	0.9983	0.10	0.18	7.17	0.95
SBA-15-E-NNN-15%	4.8	0.46	0.45	0.41	0.9994	0.09	0.17	4.62	0.94
SBA-15-C-NNN-30%	4.0	0.34	0.36	0.33	0.9998	0.08	0.17	5.67	0.94
SBA-15-PEI-30%	5.9	0.27	0.32	0.017	0.9813	0.05	0.015	1.86	0.95
SBA-15-PEI-50%	9.6	0.14	0.15	0.028	0.8625	0.02	0.001	1.07	0.82

Note: Individual adsorption experiments: 45 mL of Cd(II) aqueous solution ( $C_0 = 5\text{--}300 \text{ mg L}^{-1}$ ) and 25 mg of adsorbent.  $T = 25^\circ\text{C}$ , natural pH.

higher concentrations. Figs. S6(A) and (B) display the estimated Langmuir and Freundlich linear plots, respectively. The equilibrium data were reasonably modelled by the Langmuir equation, although the difference between both fits, Langmuir and Freundlich, summarized in Table 3, was much less significant than the ones previously observed for grafted adsorbents.

The adsorption properties of PEI-impregnated SBA-15 were found strongly depending on the impregnation percentage, but the correlation was opposite to the one expected on the basis of nitrogen content. As observed in Fig. 4 and Table 3, SBA-15-C-PEI-50% yields lower cadmium adsorption capacity than SBA-15-C-PEI-30%, in spite of the former containing much more organic nitrogen ( $9.6 \text{ mmol N g}^{-1}$ ) than the latter ( $5.9 \text{ mmol N g}^{-1}$ ). This reduction is probably due to the pore blocking effect that massive impregnation originates (Fig. 4; Table 1); hence, many amino groups become inaccessible to aqueous Cd(II) species and SBA-15-C-PEI-50% is rather inefficient for the cadmium removal. Whereas, SBA-15-C-PEI-30% adsorbent could achieve significant Cd(II) uptake ( $0.27 \text{ mmol Cd g}^{-1}$ ) under the same conditions, this cadmium adsorption capacity is similar or even higher than the one reported in literature for PEI supported on silica, which was found to be lower than the one corresponding to Pb(II) sorption [47,48,65]. Our results suggest that a fair compromise between PEI content and both tolerable mesostructure and porosity decline should be assessed to obtain suitable adsorbents for metal removal in aqueous solution.

The comparison between both types of adsorbents for cadmium, amine-grafted and PEI-impregnated, proved that grafted samples systematically yielded better results, although their nitrogen content was lower. As it can be observed in Table 3, cadmium to nitrogen molar ratio was significantly smaller (0.02 and 0.05) for impregnated materials than for the grafted materials (0.08–0.10). This fact points that the location of amino groups in PEI polymer might not be favourable to capture cadmium species or, on the contrary, the metal species in solution cannot easily access many amino active sites.

### 3.2.3. Comparison of maximum adsorption capacities with other adsorbents

The comparison of our experimental maximum adsorption capacities of aqueous lead against values found for other amine-functionalized mesoporous silica materials having similar amino groups density confirms the excellent results achieved in this work. Just to mention some examples, functionalization with AP of HMS or MCM-41 yielded Pb(II) uptake smaller than  $0.5 \text{ mmol Pb g}^{-1}$  [40,41,43] and the capacity reported for ED grafted in MCM-41 were equal to  $0.8 \text{ mmol g}^{-1}$ . DT organosilane was used as a precursor to obtain a more complex ligand for developing mesoporous silica-based lead adsorbent, but metal uptake was not greater than  $0.3 \text{ mmol Pb g}^{-1}$  [66]. Imprinting technique was used to prepare Pb(II) adsorbents with a chelating silylating agent that contained four N-donor atoms; these materials were prepared from ED organosilane and 2-pyridinecarboxaldehyde. Their reported adsorption for lead was only  $0.3 \text{ mmol Pb g}^{-1}$ , while for non-imprinted materials the maximum adsorption was  $0.20 \text{ mmol g}^{-1}$  [66]. For SBA-15, significant Pb(II) capacities were

reported for monoaminopropyl-modified adsorbents ( $0.19$  [67] and  $0.63 \text{ mmol g}^{-1}$  [68]), but smaller than that obtained here.

Other authors also described the cadmium adsorption with adsorbent based on ED and DT molecules. For instance, Cd(II)-imprinted hybrid adsorbent with DT organosilane was tested for the removal of cadmium(II) from aqueous solutions. Although the imprinted adsorbent achieved a higher adsorption capacity ( $0.68 \text{ mmol g}^{-1}$ ), the non-imprinted adsorbent capacity was  $0.42 \text{ mmol g}^{-1}$ , similar to the results presented in this work [69]. The cadmium removal ability of adsorbents grafted with ED and AP was found in literature, but reported results were divergent. In general, our SBA-15-E-NN/NNN materials achieved higher adsorption capacities than the described mesosilicas functionalized with AP [40,41], although some authors reported values close to  $0.7 \text{ mmol Cd g}^{-1}$  for AP [33] or ED grafted materials of the M41S family [43].

Therefore, the notable results for lead removal attained in this study are attributed to the presence of several amino groups within the same organic chain that is incorporated into the SBA-15 open mesostructure. Accordingly, it is noteworthy the advantage of using of SBA-15 which has larger pore diameters than other mesostructured silicas or silica gel and allows a better accessibility to active groups. Moreover, these adsorption capacities are similar to those obtained for recently presented adsorbents prepared from magnetic silica composites, which also exhibit significant capacities [70,71].

### 3.2.4. Adsorbent efficiency for lead and cadmium removal

The removal capacity at low heavy metal concentrations is one the most important criterion for selecting an adsorbent, since it is not frequent to find water streams polluted with metal concentration as high as these needed to reach the maximum adsorbent removal capacity. Thus, the goal of an adsorbent is its ability to significantly reduce the metal level to values lower than the limits established by legislation.

Fig. 5 displays the percentage of removal achieved for selected amine-grafted SBA-15 materials as a function of the initial concentration of lead (A) and cadmium (B) in the experimental conditions of this study, namely, 25 mg of adsorbent and 45 mL of solution. Said dose of adsorbent has been intentionally selected to investigate the potentiality of all the materials considered in this study as possible candidates for water decontamination. As seen, the Pb(II) uptake by any of the grafted materials yielded almost complete removal percentages even for initial lead concentration as high as  $120 \text{ mg L}^{-1}$ . It is remarkable the good performance of extracted materials that were enough efficient to reach aqueous Pb(II) concentrations under allowed values for drinking water. For instance, when treating  $30 \text{ mg L}^{-1}$  solutions with SBA-15-E-NN-15% or SBA-15-E-NNN-15% samples, the final concentration were below  $0.008 \text{ mg L}^{-1}$  (8 ppb). Nevertheless, for calcined samples, SBA-15-C-NN-30% and SBA-15-C-NNN-30%, the efficiency was slightly lower, but still notable, reaching Pb(II) removal percentage around 99% for 61.0 and  $111.3 \text{ mg L}^{-1}$  initial concentrations, respectively.

For cadmium adsorption, the efficiency of removal using grafted materials was also near 99%; however, the usable initial concentration range decreased in comparison with lead. Thus, for aqueous concentrations up to  $15 \text{ mg Cd L}^{-1}$ ,

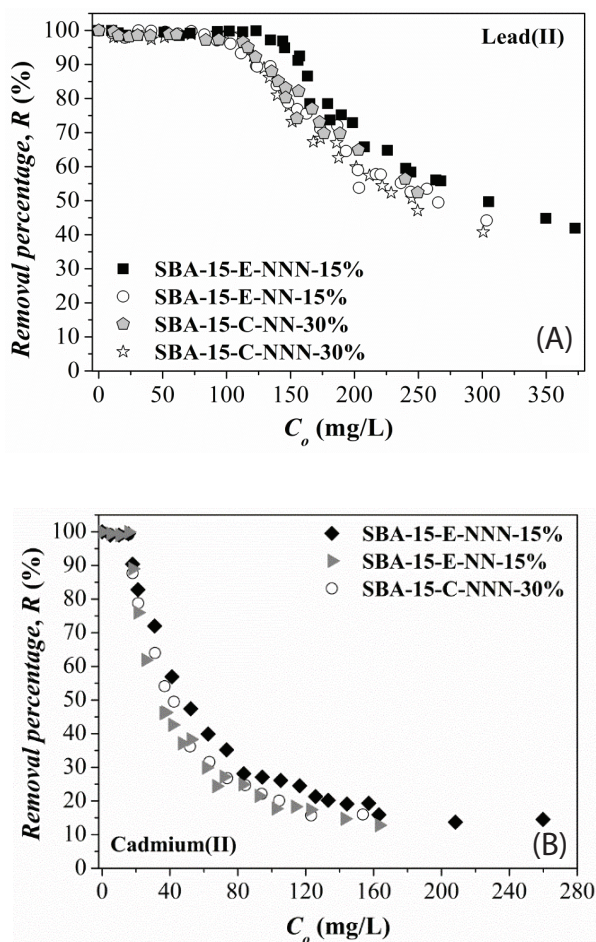


Fig. 5. Removal percentage vs. initial concentration for amine-grafted SBA-15 adsorbents. (A) Pb(II) aqueous solutions; (B) Cd(II) aqueous solutions. Ratio of adsorbent/heavy metal solution employed is  $0.56 \text{ mg mL}^{-1}$ , which means 25 mg of adsorbent per 45 mL of heavy metal solution.

the uptake percentage ranged from 99.4 to 99.9 for SBA-15-E-NNN-15% and SBA-15-E-NN-15%, respectively, being possible to attain final Cd concentrations under  $0.01 \text{ mg L}^{-1}$  (10 ppb) with the latter.

The experimental data obtained in this work evidence that amine-grafted adsorbents were suitable for treating contaminated water with lead or cadmium and for reducing the pollutant levels below the authorized limits. Conversely, Cd(II) removal by PEI impregnated materials was significantly poorer with percentages around 21% for  $25 \text{ mg Cd L}^{-1}$  initial concentration.

To conclude this section, it must be emphasized that the adsorbent mass to solution volume ratio selected for experiments was comparatively low in this study, lesser than  $1 \text{ g L}^{-1}$ . Amine-grafted SBA-15 materials were able to remove almost 100% of lead when treating  $125 \text{ mg L}^{-1}$  solutions and so did they for cadmium, although at lower initial concentration. However, the amount of adsorbent found in literature for materials capable of reaching almost complete metal removal was significantly higher. For example, a lead removal of 95%–97% was reported for AP-MCM-41 treating  $50 \text{ mg L}^{-1}$  solutions, but the experimental mass/volume ratio

was  $5 \text{ g L}^{-1}$  [41]; while SBA-15-E-NNN-15% prepared in the present work can remove more than 99.5% using a mass/volume ratio 10 times smaller ( $0.56 \text{ g L}^{-1}$ ).

### 3.2.5. Adsorption mechanism

It has been widely proposed in literature that the plausible mechanism involved in the adsorption of lead or cadmium on amine compounds is metal complexation. The significant differences between both metals could be explained in terms of the hard-soft acid–base theory describing the mutual affinity of metals and ligand when forming complexes [72]. According to this theory, the Lewis acids and bases are divided into hard or soft species, with hard acids reacting preferentially with hard bases, and soft acids preferentially with soft bases. Acids of intermediate case could bond either with hard and soft bases. Metallic cations behave as acids, being harder, in general, as the polarizability decreases, while nitrogen in aliphatic amino groups acts as hard base. Thus, as cationic  $\text{Cd}^{2+}$  is a soft acid and  $\text{Pb}^{2+}$  is a border line acid [72], the affinity of amino groups of AP, ED, or DT molecules must be higher for lead. Likewise, for other types of ligands such as melamine-based dendrimer amines having both aromatic and aliphatic amines, the lead adsorption is higher than cadmium adsorption [21]. Since complexation is the main mechanism to explain the aqueous lead(II) adsorption by amine-functionalized silica adsorbents, the involvement of amino and silanol groups as ligands should be evaluated. As seen in Table 2, the molar ratio calculated as maximum adsorbed Pb(II) related to nitrogen content ( $Q_{\text{max}}/N$ ) decreased from 0.32–0.36 for ED(NN) adsorbents to 0.27–0.28 for DT(NNN). Therefore, the nitrogen presented in ED chains was more efficient for adsorption. Accordingly, while around three nitrogen positions were necessary per each Pb(II) species with ED molecules, 3.6 nitrogen atoms were computed for each  $\text{Pb}^{2+}$  ion in the case of DT adsorbents. In terms of loaded organosilane, one lead entity required around 1.40–1.47 ED(NN) and 1.17–1.21 DT(NNN) organic chains, suggesting that the formed complex could be explained considering three or four nitrogen positions, respectively. However, it is difficult to establish the metal coordination because some amino functional groups of the silica structure could be inaccessible for metallic species or located at longer distance than required.

Another likely factor that could avoid the metal–nitrogen interaction could be the nitrogen–hydrogen bonding of adjacent amino groups which can be favoured with the increase of the alkyl chain length and density of amino-organic moieties [61]. Moreover, oxygen atoms of silanol groups hypothetically could also be involved in the complex formation. The presence of these groups on the adsorbents surface has been evidenced by  $^{29}\text{Si}$  MAS-NMR (peaks  $Q^2$  and  $Q^3$  in Fig. 3), and it has been reported that lead exhibit some affinity to ligands containing nitrogen and oxygen [22,23]. It is interesting to mention here that when EDTA is used to modify the SBA-15 surface, it was found that lead adsorption could be a complex process involving ion exchange and surface complexation through amino groups and oxygen of carboxyl groups, with the latter being dominant [24].

Regarding cadmium, the maximum adsorption capacity found for any of the amine-grafted materials was smaller than the value determined for lead. Actually, the molar cadmium

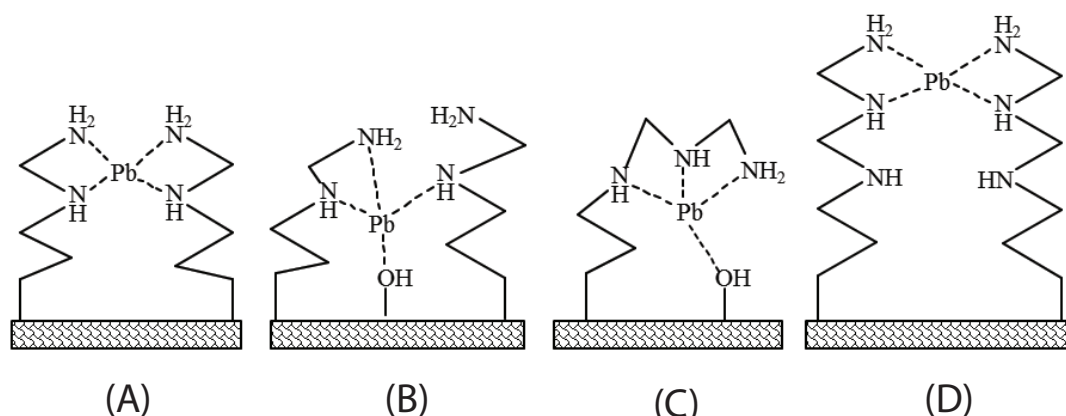


Fig. 6. Hypothesized coordination structures for lead adsorption on NN ((A) and (B)) and NNN ((C) and (D)).

to nitrogen ratio is at the most 0.1, pointing that each cadmium species would need 10 nitrogen sites to be adsorbed. This ratio reveals a smaller chemical affinity of cadmium to nitrogen that reduces the metal tendency to form aminated complexes. Surface complexation was also reported for cadmium adsorption on silica gel and zeolites functionalized with propylethylenediamine triacetic acid trisodium salt. Here, mononuclear and polynuclear complexes involving nitrogen and oxygen were proposed being formed even with the participation of silanol groups [73]. EDTA has also been studied, although the affinity was found to be smaller than that of lead due to the smaller equilibrium constant [25].

The metal to nitrogen ratio determined for lead (Table 2) is in agreement with the well-established Pb(II) tendency to form tetra-linked complexes, preferentially with hemidirected coordination geometry [74]. However, many different coordination structures involving four nitrogen atoms could be understood depending on the number of amino groups and their proximity, as displayed in Fig. 6, where the possible involvement of silanol groups in the complex formation is included. In any case, it should be pointed out that the adsorption of Pb<sup>2+</sup> on SBA-15 pure silica, that contains many free surface silanol groups, is negligible [75].

To deepen in the metal complexation mechanism and underline the differences between lead and cadmium, the shift of the pH solution value was measured for every experiment. Fig. 7 displays the pH values of the aqueous metal solutions determined before and after adsorption on SBA-15-E-NNN-15% for Pb(II) and Cd(II). Within the range of initial concentration shown in the figure, that is, up to 225 mg L<sup>-1</sup>, the natural pH of both metal solutions thoroughly was around 5.5, except for low concentration where it increased to 6–7. Although the pH dependence of aqueous metal speciation is troublesome, especially for lead at pH > 7 [76], the weak acid behaviour observed can be mainly attributed to minor hydrolysis of Pb<sup>2+</sup> and Cd<sup>2+</sup> ions through the processes:



According to the speciation diagrams calculated using the chemical equilibrium modelling software MINEQL+ [77],

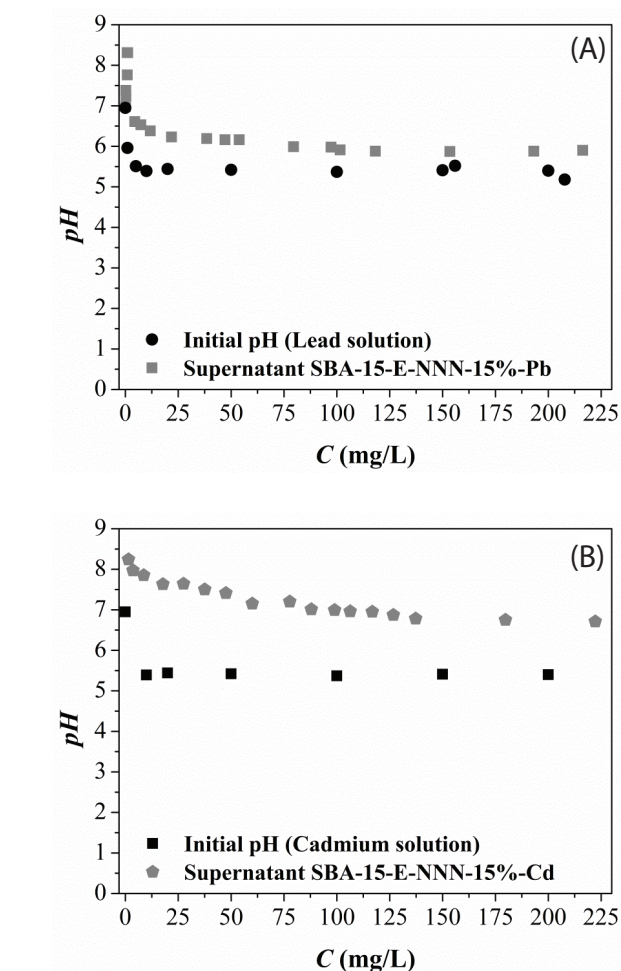
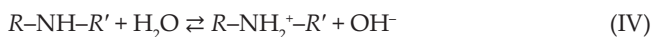


Fig. 7. Experimental pH of aqueous Pb(II) and Cd(II) solutions measured before and after adsorption on SBA-15-E-NNN-15%.

the aqueous divalent cations Cd<sup>2+</sup> and Pb<sup>2+</sup> are the only metallic species expected in solution, along with lower amounts of the soluble monohydroxides Pb(OH)<sup>+</sup> and Cd(OH)<sup>+</sup>, under initial conditions [75].

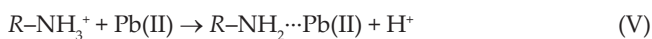
After adsorption with amine-functionalized SBA-15, the solution pH systematically raised as observed in Fig. 7.

It must be emphasized that the adsorbent addition to pure water also increased the pH due to amino groups that are partially protonated in water, as previously reported for similar materials [78]:



Therefore, the pH change accompanying the adsorption could be interpreted as a mere acid–base neutralization process. However, this simple explanation is unsatisfactory due to the difference observed between Pb(II) and Cd(II). Save for dilute solutions, the pH increase is significantly lower with lead than with cadmium. Taking into account that adsorption extent is higher for lead, the pH alteration should be related to the metal capture. By assuming, as explained earlier (Fig. 6), that the main adsorption mechanism is metal complexation to non-protonated amino groups, the evident conclusion is that the binding of Pb(II) ions to many nitrogen atoms of the amine chains prevents their further protonation through hydrolysis, unless too low lead concentration is used. Conversely, since the cadmium adsorption on amino groups is less effective, the lone electron pairs of many nitrogen atoms remain free for protonation.

Of course, the same conclusion would be attained if looking the process as the pH reduction promoted by the addition of metal ions to basic solutions that contain the adsorbent. Accordingly, chemisorption would resemble an ion-exchange process of the following type:



It should be mentioned that the acid–base behaviour of the residual silanol groups existing on the adsorbent surface has not been discussed in this work. This is a relevant but cumbersome issue; nevertheless, no significant contribution is attributed to this cause, since the Si–OH groups are inactive within the pH range under study where neither protonation nor dissociation is expected [79].

As final remark, it must be commented that the pH influence on cadmium and lead adsorption has been widely studied for amine-functionalized adsorbents [40,42,44,80]. By restricting to acidic conditions to prevent precipitation of insoluble species, the prevalent conclusion that could be drawn suggest that the adsorption degree dramatically diminishes below pH = 4 due to amino groups' protonation that hinders the lone electron pair belonging to the nitrogen, creates a repulsing surface to cations, and inhibits the complexation process with Pb<sup>2+</sup> or Cd<sup>2+</sup> ions. We have found a similar tendency in explorative experiments carried out with SBA-15-E-NNN-15% in HNO<sub>3</sub> medium that confirms the inefficiency of the prepared adsorbents in moderate and strong acidic conditions.

#### 4. Conclusions

Mesoporous silica materials type SBA-15 functionalized with multiamine chains have been successfully prepared for selective adsorption of aqueous Pb(II) and Cd(II) contaminants. Calcined and extracted SBA-15 supports have been grafted with different percentages of organic chains containing amino

groups (ethylenediamine and diethylenetriamine). In addition, calcined SBA-15 has also been impregnated with a heavily loaded polymer with amino groups (PEI). All the prepared materials present adequate stability and textural properties to act as adsorbents in aqueous media. Lead(II) and cadmium(II) adsorption studies has been conducted up to saturation point to obtain the full isotherms that are satisfactorily modelled by the Langmuir equation. All adsorbents are efficient at low metal concentration with removal percentages higher than 99%, yielding concentration values which are below legally stabilised threshold. SBA-15-E-NNN-15%, the best prepared material, exhibits maximum adsorption capacities as high as 1.37 mmol g<sup>-1</sup> (284 mg g<sup>-1</sup>) and 0.46 mmol g<sup>-1</sup> (50.6 mg g<sup>-1</sup>) for lead and cadmium, respectively. This material also renders full capacity of decontamination even when exposed to initial high concentrations of metals (140 mg Pb(II) L<sup>-1</sup> and 21 mg Cd(II) L<sup>-1</sup>). These values are uncommonly high when compared with those reported in literature for most specific adsorbents whose synthesis is usually more intricate. Especially for Pb(II), it is achievable to reduce the toxic metal concentration below the legally authorised levels in drinking water employing uncommonly low dosages (0.56 g L<sup>-1</sup>). Finally, this study demonstrates that the incorporation of an excessively large organic content to the silica support can be unfavourable for sorption purposes, since PEI-impregnated materials having the highest nitrogen content exhibited the worst efficacy for cadmium uptake. These adsorbents could potentially be used in real world water samples contaminated at a trace level. In particular, SBA-15-E-NNN-15% is a promising candidate for water purification applications, singularly for purification in flow processes.

#### Acknowledgements

This work was supported by the Ministerio de Economía y Competitividad of Spanish Government, and Regional Government of Madrid through the research projects CTM2015-69246-R and Proyecto S2013/MAE-2716-REMTAVARES-CM, respectively. The authors would like to thank Mr. Carlos Isam Bachour Simerol for his valuable assistance in English writing.

#### Symbols

SBA-15-C	–	Calcined SBA-15 (surfactant eliminated by calcination)
SBA-15-E	–	Extracted SBA-15 (surfactant eliminated by extraction)
AP or N	–	Aminopropyl
ED or NN	–	ethylenediamine
DT or NNN	–	diethylenetriamine
PEI	–	Polyethylenimine
$D_p$	–	BJH pore diameter
$S_{BET}^p$	–	BET surface area
$V_p$	–	Pore volume
$d_{100}^p$	–	Interplanar distance in the (100) planes
$a_0$	–	Unit cell parameter calculated as $a_0 = \frac{2 \cdot d_{100}^p}{\sqrt{3}}$
$e_p$	–	Silica wall thickness estimated as $e_p = a_0 - D_p$

## References

- [1] WHO, Guidelines for Drinking-Water Quality: Fourth Edition Incorporating the First Addendum, 4th ed., World Health Organization, Geneva, 2017.
- [2] USEPA (EPA), How EPA Regulates Drinking Water Contaminants, 2018. Available at: <https://www.epa.gov/dwregdev/how-epa-regulates-drinking-water-contaminants> (Accessed 03 November 2018).
- [3] USEPA, Integrated Science Assessment for Lead (Third External Review Draft), United States Environmental Protection Agency, Washington, DC, 2012.
- [4] L. Fewtrell, R. Kaufmann, A. Prüss-Üstün, In: Lead. Assessing the Environmental Burden of Disease at National and Local Level, in A. Prüss-Üstün, D. Campbell-Lendrum, C. Corvalán, A. Woodward, Eds., WHO Environmental Burden of Disease Series, No. 2, World Health Organization, Geneva, Switzerland, 2003, p. 73.
- [5] C.B. United Nations Environment Programme, DTIE, Final Review of Scientific Information on Cadmium, 2010, p. 324.
- [6] M. Jaishankar, T. Tseten, N. Anbalagan, B.B. Mathew, K.N. Beeregowda, Toxicity, mechanism and health effects of some heavy metals, *Interdiscip. Toxicol.*, 7 (2014) 60–72.
- [7] Directive 2008/105/EC of the European Parliament and of the Council of 16 December 2008 on Environmental Quality Standards in the Field of Water Policy, Amending and Subsequently Repealing Council Directives 82/176/EEC, 83/513/EEC, 84/156/EEC, 84/491/EEC, 86/280/EEC and Amending Directive 2000/60/EC of the European Parliament and of the Council, 2008.
- [8] Directive 2013/39/EU of the European Parliament and of the Council of 12 August 2013 Amending Directives 2000/60/EC and 2008/105/EC as Regards Priority Substances in the Field of Water Policy, 2013.
- [9] Opinion of the European Economic and Social Committee on the 'Proposal for a Directive of the European Parliament and of the Council amending Directives 2000/60/EC and 2008/105/EC as Regards Priority Substances in the Field of Water Policy' COM(2011) 876 final – 2011/0429 (COD) 2012.
- [10] N.P. Cheremisinoff, Handbook of Water and Wastewater Treatment Technologies, Butterworth-Heinemann, 2002.
- [11] P. Jovančić, M. Radetić, Advanced Sorbent Materials for Treatment of Wastewaters, in Handbook of Environmental Chemistry, Vol. 5, 2008, pp. 239–264.
- [12] V.K. Gupta, A. Nayak, B. Bhushan, S. Agarwal, A critical analysis on the efficiency of activated carbons from low-cost precursors for heavy metals remediation, *Crit. Rev. Environ. Sci. Technol.*, 45 (2015) 613–668.
- [13] A. Walcarius, L. Mercier, Mesoporous organosilica adsorbents: nanoengineered materials for removal of organic and inorganic pollutants, *J. Mater. Chem.*, 20 (2010) 4478–4511.
- [14] X. Feng, G.E. Fryxell, L.Q. Wang, A.Y. Kim, J. Liu, K.M. Kemner, Functionalized monolayers on ordered mesoporous supports, *Science*, 276 (1997) 923–926.
- [15] J. Aguado, J.M. Arsuaga, A. Arencibia, Adsorption of aqueous mercury(II) on propylthiol-functionalized mesoporous silica obtained by cocondensation, *Ind. Eng. Chem. Res.*, 44 (2005) 3665–3671.
- [16] A.M. Liu, K. Hidajat, S. Kawi, D.Y. Zhao, A new class of hybrid mesoporous materials with functionalized organic monolayers for selective adsorption of heavy metal ions, *Chem. Commun.*, (2000) 1145–1146.
- [17] Y. Jiang, Q. Gao, H. Yu, Y. Chen, F. Deng, Intensively competitive adsorption for heavy metal ions by PAMAM-SBA-15 and EDTA-PAMAM-SBA-15 inorganic-organic hybrid materials, *Microporous Mesoporous Mater.*, 103 (2007) 316–324.
- [18] A. Shahbazi, H. Younesi, A. Badiei, Batch and fixed-bed column adsorption of Cu(II), Pb(II) and Cd(II) from aqueous solution onto functionalised SBA-15 mesoporous silica, *Can. J. Chem. Eng.*, 91 (2013) 739–750.
- [19] L.C.C.d. Silva, L.B.O.d. Santos, G. Abate, I.C. Cosentino, M.C.A. Fantini, J.C. Masini, J.R. Matos, Adsorption of Pb<sup>2+</sup>, Cu<sup>2+</sup> and Cd<sup>2+</sup> in FDU-1 silica and FDU-1 silica modified with humic acid, *Microporous Mesoporous Mater.*, 110 (2008) 250–259.
- [20] L. Hajiaghbabaei, T. Tajmiri, A. Badiei, M.R. Ganjali, Y. Khaniani, G.M. Ziarani, Heavy metals determination in water and food samples after preconcentration by a new nanoporous adsorbent, *Food Chem.*, 141 (2013) 1916–1922.
- [21] A. Shahbazi, H. Younesi, A. Badiei, Functionalized SBA-15 mesoporous silica by melamine-based dendrimer amines for adsorptive characteristics of Pb(II), Cu(II) and Cd(II) heavy metal ions in batch and fixed bed column, *Chem. Eng. J.*, 168 (2011) 505–518.
- [22] Y. Liu, Z. Liu, J. Gao, J. Dai, J. Han, Y. Wang, J. Xie, Y. Yan, Selective adsorption behavior of Pb(II) by mesoporous silica SBA-15-supported Pb(II)-imprinted polymer based on surface molecularly imprinting technique, *J. Hazard. Mater.*, 186 (2011) 197–205.
- [23] G. Ye, F. Bai, G. Chen, J. Wei, J. Wang, J. Chen, A novel well-ordered mesoporous organosilica specialized for highly selective recognition of Pb(II) by host-guest interactions, *J. Mater. Chem.*, 22 (2012) 20878–20880.
- [24] J. Huang, M. Ye, Y.Q. Qu, L.F. Chu, R. Chen, Q.Z. He, D.F. Xu, Pb (II) removal from aqueous media by EDTA-modified mesoporous silica SBA-15, *J. Colloid Interface Sci.*, 385 (2012) 137–146.
- [25] Z. Ezzeddine, I. Batonneau-Gener, Y. Pouilloux, H. Hamad, Z. Saad, V. Kazpard, Divalent heavy metals adsorption onto different types of EDTA-modified mesoporous materials: effectiveness and complexation rate, *Microporous Mesoporous Mater.*, 212 (2015) 125–136.
- [26] Z. Gao, L. Wang, T. Qi, J. Chu, Y. Zhang, Synthesis, characterization, and cadmium(II) uptake of iminodiacetic acid-modified mesoporous SBA-15, *Colloids Surf., A*, 304 (2007) 77–81.
- [27] A. Benhamou, M. Baudu, Z. Derriche, J.P. Basly, Aqueous heavy metals removal on amine-functionalized Si-MCM-41 and Si-MCM-48, *J. Hazard. Mater.*, 171 (2009) 1001–1008.
- [28] A. Sayari, S. Hamoudi, Y. Yang, Applications of pore-expanded mesoporous silica. 1. Removal of heavy metal cations and organic pollutants from wastewater, *Chem. Mater.*, 17 (2005) 212–216.
- [29] L. Zhang, C. Yu, W. Zhao, Z. Hua, H. Chen, L. Li, J. Shi, Preparation of multi-amine-grafted mesoporous silicas and their application to heavy metal ions adsorption, *J. Non-Cryst. Solids*, 353 (2007) 4055–4061.
- [30] L. Bois, A. Bonhomme, A. Ribes, B. Pais, G. Raffin, F. Tessier, Functionalized silica for heavy metal ions adsorption, *Colloids Surf., A*, 221 (2003) 221–230.
- [31] T. Yokoi, H. Yoshitake, T. Tatsumi, Synthesis of amino-functionalized MCM-41 via direct co-condensation and post-synthesis grafting methods using mono-, di- and tri-amino-organoalkoxysilanes, *J. Mater. Chem.*, 14 (2004) 951–957.
- [32] K.F. Lam, K.L. Yeung, G. McKay, A rational approach in the design of selective mesoporous adsorbents, *Langmuir*, 22 (2006) 9632–9641.
- [33] K.F. Lam, K.L. Yeung, G. McKay, Efficient approach for Cd<sup>2+</sup> and Ni<sup>2+</sup> removal and recovery using mesoporous adsorbent with tunable selectivity, *Environ. Sci. Technol.*, 41 (2007) 3329–3334.
- [34] E. Da'na, A. Sayari, Adsorption of heavy metals on amine-functionalized SBA-15 prepared by co-condensation: applications to real water samples, *Desalination*, 285 (2012) 62–67.
- [35] M. Algarra, M.V. Jimenez, E. Rodriguez-Castellon, A. Jimenez-Lopez, J. Jimenez-Jimenez, Heavy metals removal from electroplating wastewater by aminopropyl-Si MCM-41, *Chemosphere*, 59 (2005) 779–786.
- [36] H. Lee, J. Yi, Removal of copper ions using functionalized mesoporous silica in aqueous solution, *Sep. Sci. Technol.*, 36 (2001) 2433–2448.
- [37] K.F. Lam, X. Chen, G. McKay, K.L. Yeung, Anion effect on Cu<sup>2+</sup> adsorption on NH<sub>2</sub>-MCM-41, *Ind. Eng. Chem. Res.*, 47 (2008) 9376–9383.
- [38] M.V. Lombardo, M. Videla, A. Calvo, F.G. Requejo, G.J. Soler-Illia, Aminopropyl-modified mesoporous silica SBA-15 as

- recovery agents of Cu(II)-sulfate solutions: adsorption efficiency, functional stability and reusability aspects, *J. Hazard. Mater.*, 223–224 (2012) 53–62.
- [39] L. Giraldo, J.C. Moreno-Piraján, Study on the adsorption of heavy metal ions from aqueous solution on modified SBA-15, *Mater. Res-Ibero-Am. J.*, 16 (2013) 745–754.
- [40] M. Machida, B. Fotoohi, Y. Amamo, L. Mercier, Cadmium(II) and lead(II) adsorption onto hetero-atom functional mesoporous silica and activated carbon, *Appl. Surf. Sci.*, 258 (2012) 7389–7394.
- [41] A. Heidari, H. Younesi, Z. Mehraban, Removal of Ni(II), Cd(II), and Pb(II) from a ternary aqueous solution by amino functionalized mesoporous and nano mesoporous silica, *Chem. Eng. J.*, 153 (2009) 70–79.
- [42] V. Hernández-Morales, R. Nava, Y.J. Acosta-Silva, S.A. Macías-Sánchez, J.J. Pérez-Bueno, B. Pawelec, Adsorption of lead(II) on SBA-15 mesoporous molecular sieve functionalized with  $-NH_2$  groups, *Microporous Mesoporous Mater.*, 160 (2012) 133–142.
- [43] H. Faghiani, M. Naghavi, Synthesis of amine-functionalized MCM-41 and MCM-48 for removal of heavy metal ions from aqueous solutions, *Sep. Sci. Technol.*, 49 (2014) 214–220.
- [44] M. Machida, B. Fotoohi, Y. Amamo, T. Ohba, H. Kanoh, L. Mercier, Cadmium(II) adsorption using functional mesoporous silica and activated carbon, *J. Hazard. Mater.*, 221–222 (2012) 220–227.
- [45] K. Xia, R.Z. Ferguson, M. Losier, N. Tchoukanova, R. Bruning, Y. Djaoued, Synthesis of hybrid silica materials with tunable pore structures and morphology and their application for heavy metal removal from drinking water, *J. Hazard. Mater.*, 183 (2010) 554–564.
- [46] J. Aguado, J.M. Arsuaga, A. Arencibia, M. Lindo, V. Gascon, Aqueous heavy metals removal by adsorption on amine-functionalized mesoporous silica, *J. Hazard. Mater.*, 163 (2009) 213–221.
- [47] M. Ghoul, M. Bacquet, M. Morcellet, Uptake of heavy metals from synthetic aqueous solutions using modified PEI–silica gels, *Water Res.*, 37 (2003) 729–734.
- [48] B. Gao, F. An, K. Liu, Studies on chelating adsorption properties of novel composite material polyethyleneimine/silica gel for heavy-metal ions, *Appl. Surf. Sci.*, 253 (2006) 1946–1952.
- [49] D.Y. Zhao, Q.S. Huo, J.L. Feng, B.F. Chmelka, G.D. Stucky, Nonionic triblock and star diblock copolymer and oligomeric surfactant syntheses of highly ordered, hydrothermally stable, mesoporous silica structures, *J. Am. Chem. Soc.*, 120 (1998) 6024–6036.
- [50] D.Y. Zhao, J.L. Feng, Q.S. Huo, N. Melosh, G.H. Fredrickson, B.F. Chmelka, G.D. Stucky, Triblock copolymer syntheses of mesoporous silica with periodic 50 to 300 angstrom pores, *Science*, 279 (1998) 548–552.
- [51] R. Sanz, G. Calleja, A. Arencibia, E.S. Sanz-Pérez,  $CO_2$  adsorption on branched polyethyleneimine-impregnated mesoporous silica SBA-15, *Appl. Surf. Sci.*, 256 (2010) 5323–5328.
- [52] K.S.W. Sing, Reporting physisorption data for gas/solid systems with special reference to the determination of surface area and porosity (Recommendations 1984), *Pure Appl. Chem.*, 57 (1985) 603–619.
- [53] H. Vojoudi, A. Badieli, S. Bahar, G. Mohammadi Ziarani, F. Faridbod, M.R. Ganjali, Post-modification of nanoporous silica type SBA-15 by bis(3-triethoxysilylpropyl)tetrasulfide as an efficient adsorbent for arsenic removal, *Powder Technol.*, 319 (2017) 271–278.
- [54] S. Kim, S. Park, S. Han, Y. Han, J. Park, Silanol-rich ordered mesoporous silica modified thiol group for enhanced recovery performance of Au(III) in acidic leachate solution, *Chem. Eng. J.*, 351 (2018) 1027–1037.
- [55] A.C. Voegtlin, F. Ruch, J.L. Guth, J. Patarin, L. Huve,  $F^-$  mediated synthesis of mesoporous silica with ionic- and non-ionic surfactants. A new templating pathway, *Microporous Mater.*, 9 (1997) 95–105.
- [56] E. Sanz,  $CO_2$  Capture by Mesostructured Silica Materials Functionalized with Amino Groups, Ph.D. Dissertation, Universidad Rey Juan Carlos (URJC), Department of Energy and Chemical Technology, Mostoles (Madrid), 2013.
- [57] J. Aguado, J.M. Arsuaga, A. Arencibia, Influence of synthesis conditions on mercury adsorption capacity of propylthiol functionalized SBA-15 obtained by co-condensation, *Microporous Mesoporous Mater.*, 109 (2008) 513–524.
- [58] C.H. Giles, T.H. MacEwan, S.N. Nakhwa, D. Smith, 786. Studies in adsorption. Part XI. A system of classification of solution adsorption isotherms, and its use in diagnosis of adsorption mechanisms and in measurement of specific surface areas of solids, *J. Chem. Soc.*, (1960) 3973–3993.
- [59] I. Langmuir, The adsorption of gases on plane surfaces of glass, mica and platinum, *J. Am. Chem. Soc.*, 40 (1918) 1361–1403.
- [60] H. Freundlich, Of the adsorption of gases. Section II. Kinetics and energetics of gas adsorption. Introductory paper to section II, *T. Faraday Soc.*, 28 (1932) 195–201.
- [61] M.W. McKittrick, C.W. Jones, Toward single-site functional materials-preparation of amine-functionalized surfaces exhibiting site-isolated behavior, *Chem. Mater.*, 15 (2003) 1132–1139.
- [62] R. Sanz, G. Calleja, A. Arencibia, E.S. Sanz-Pérez, Development of high efficiency adsorbents for  $CO_2$  capture based on a double-functionalization method of grafting and impregnation, *J. Mater. Chem. A*, 1 (2013) 1956–1962.
- [63] A. Heydari-Gorji, Y. Belmabkhout, A. Sayari, Polyethyleneimine-impregnated mesoporous silica: effect of amine loading and surface alkyl chains on  $CO_2$  adsorption, *Langmuir*, 27 (2011) 12411–12416.
- [64] S. Choi, M.L. Gray, C.W. Jones, Amine-tethered solid adsorbents coupling high adsorption capacity and regenerability for  $CO_2$  capture from ambient air, *ChemSusChem*, 4 (2011) 628–635.
- [65] L. He, D.D. Liu, B.B. Wang, H.B. Xu, Adsorption of lead(II) from aqueous solution using a poly(ethyleneimine)-functionalized organic-inorganic hybrid silica prepared by hydrothermal-assisted surface grafting method, *Asia-Pac. J. Chem. Eng.*, 9 (2014) 800–809.
- [66] H.T. Fan, X.T. Sun, Z.G. Zhang, W.X. Li, Selective removal of lead(II) from aqueous solution by an ion-imprinted silica sorbent functionalized with chelating N-donor atoms, *J. Chem. Eng. Data*, 59 (2014) 2106–2114.
- [67] C. McManamon, A.M. Burke, J.D. Holmes, M.A. Morris, Amine-functionalised SBA-15 of tailored pore size for heavy metal adsorption, *J. Colloid Interface Sci.*, 369 (2012) 330–337.
- [68] G. Li, B.D. Wang, Q. Sun, W.Q. Xu, Y.F. Han, Adsorption of lead ion on amino-functionalized fly-ash-based SBA-15 mesoporous molecular sieves prepared via two-step hydrothermal method, *Microporous Mesoporous Mater.*, 252 (2017) 105–115.
- [69] J.B. Wu, Y.L. Yi, Removal of cadmium from aqueous solution by organic-inorganic hybrid sorbent combining sol-gel processing and imprinting technique, *Korean J. Chem. Eng.*, 30 (2013) 1111–1118.
- [70] Q. Yuan, Y. Chi, N.S. Yu, Y. Zhao, W.F. Yan, X.T. Li, B. Dong, Amino-functionalized magnetic mesoporous microspheres with good adsorption properties, *Mater. Res. Bull.*, 49 (2014) 279–284.
- [71] P.N.E. Diagboya, E.D. Dikio, Silica-based mesoporous materials; emerging designer adsorbents for aqueous pollutants removal and water treatment, *Microporous Mesoporous Mater.*, 266 (2018) 252–267.
- [72] R.G. Pearson, Hard and soft acids and bases, *J. Am. Chem. Soc.*, 85 (1963) 3533–3539.
- [73] A.N. Vasiliev, L.V. Golovko, V.V. Trachevsky, G.S. Hall, J.G. Khinast, Adsorption of heavy metal cations by organic ligands grafted on porous materials, *Microporous Mesoporous Mater.*, 118 (2009) 251–257.
- [74] L. Shimoni-Livny, J.P. Glusker, C.W. Bock, Lone pair functionality in divalent lead compounds, *Inorg. Chem.*, 37 (1998) 1853–1867.
- [75] J. Aguado, J.M. Arsuaga, A. Arencibia, Heavy metals removal from water by adsorption on propylthiol-functionalized mesoporous silica obtained by co-condensation, *Int. J. Environ. Technol. Manage.*, 12 (2010) 381–392.
- [76] Q. Liu, Y. Liu, Distribution of Pb(II) species in aqueous solutions, *J. Colloid Interface Sci.*, 268 (2003) 266–269.

- [77] W.D. Schecher, D.C. McAwoy, MINEQL+: A Chemical Equilibrium Modeling System, Hallowell, ME, Environmental Research Software, 2001.
- [78] E. Da'na, A. Sayari, Effect of regeneration conditions on the cyclic performance of amine-modified SBA-15 for removal of copper from aqueous solutions: composite surface design methodology, *Desalination*, 277 (2011) 54–60.
- [79] K. Leung, I.M. Nielsen, L.J. Criscenti, Elucidating the bimodal acid-base behavior of the water-silica interface from first principles, *J. Am. Chem. Soc.*, 131 (2009) 18358–18365.
- [80] C. Liu, R. Bai, Q. San Ly, Selective removal of copper and lead ions by diethylenetriamine-functionalized adsorbent: behaviors and mechanisms, *Water Res.*, 42 (2008) 1511–1522.

## Supplementary material

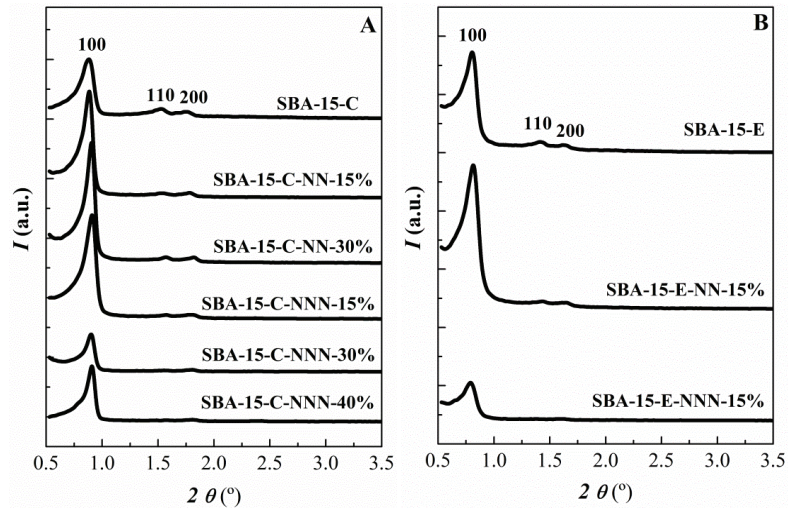


Fig. S1. Low-angle XRD patterns of pure SBA-15 and materials grafted with NN and NNN chains. (A) Calcined silica, SBA-15-C; (B) extracted silica, SBA-15-E.

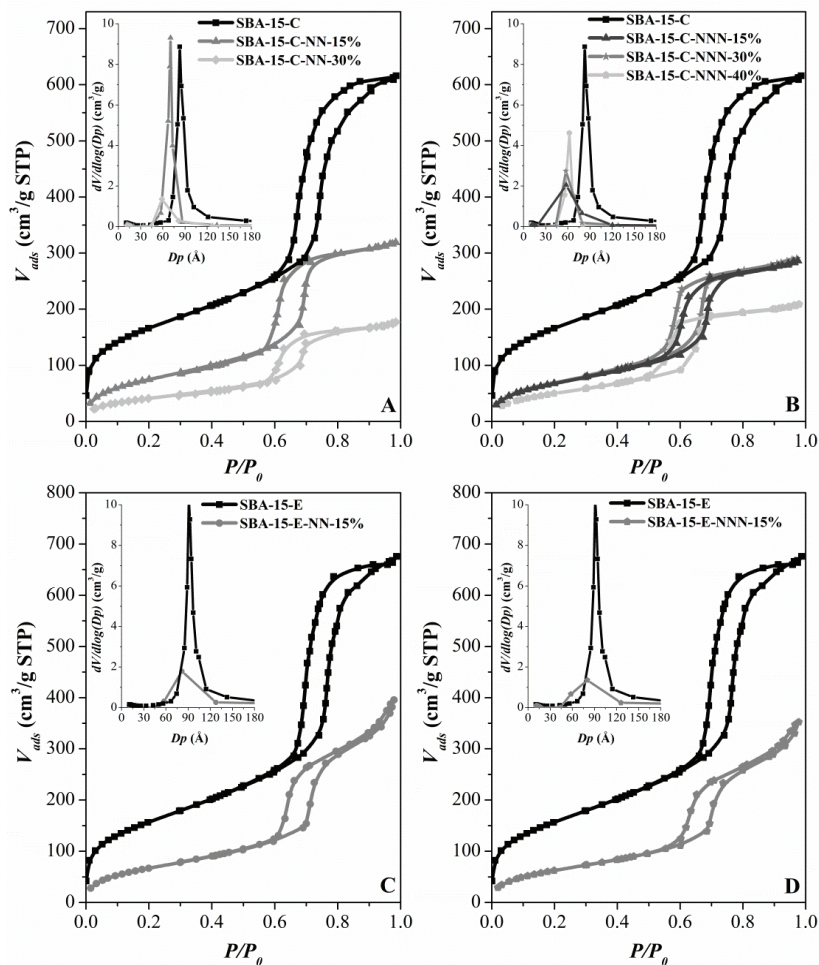


Fig. S2. Nitrogen adsorption-desorption isotherms at 77 K and BJH pore size distributions of calcined SBA-15 and materials grafted with NN (A) and NNN (B) chains, along with extracted SBA-15 and materials grafted with NN (C) and NNN (D) chains.

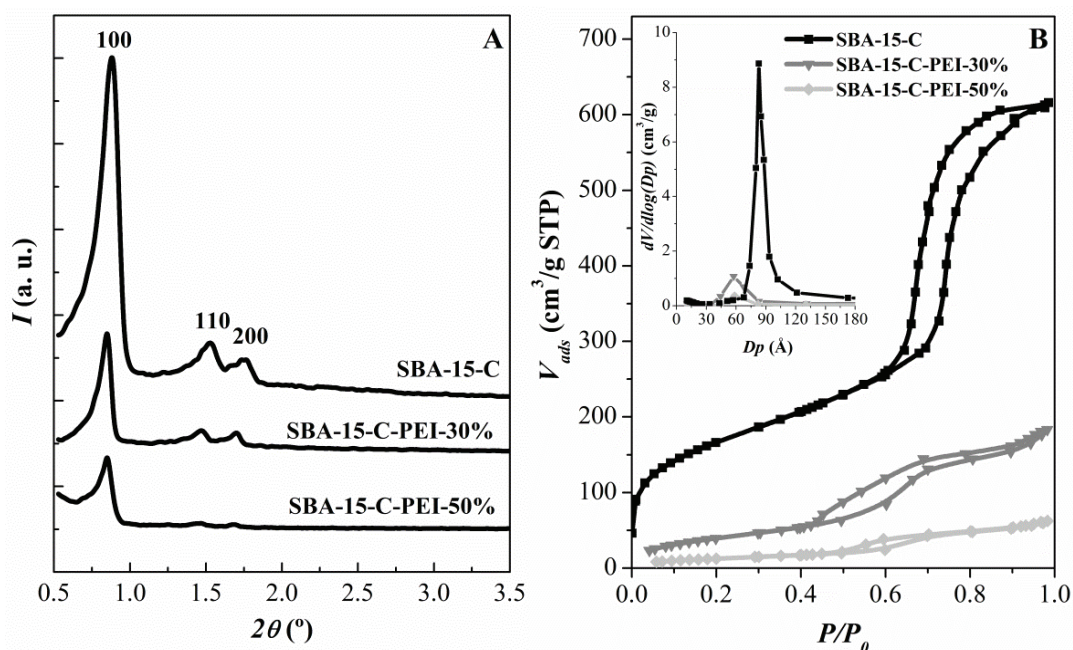


Fig. S3. (A) Low-angle XRD patterns of SBA-15-C materials impregnated with PEI. (B) Nitrogen adsorption–desorption isotherms at 77 K and BJH pore size distributions of calcined SBA-15 materials impregnated with PEI.

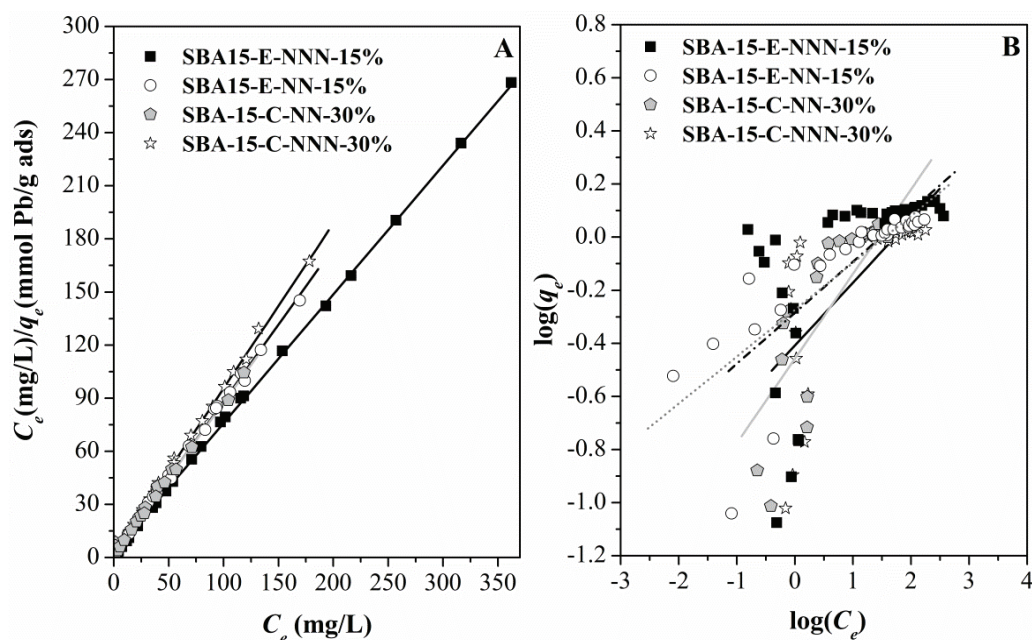


Fig. S4. (A) Linearized Langmuir isotherm plot for adsorption of lead(II) on extracted 'E' and calcined 'C' SBA-15 materials functionalized by grafting with NN and NNN organic chains. (B) Linearized Freundlich isotherm plot for adsorption of lead(II) on extracted 'E' and calcined 'C' SBA-15 materials functionalized by grafting with NN and NNN organic chains.

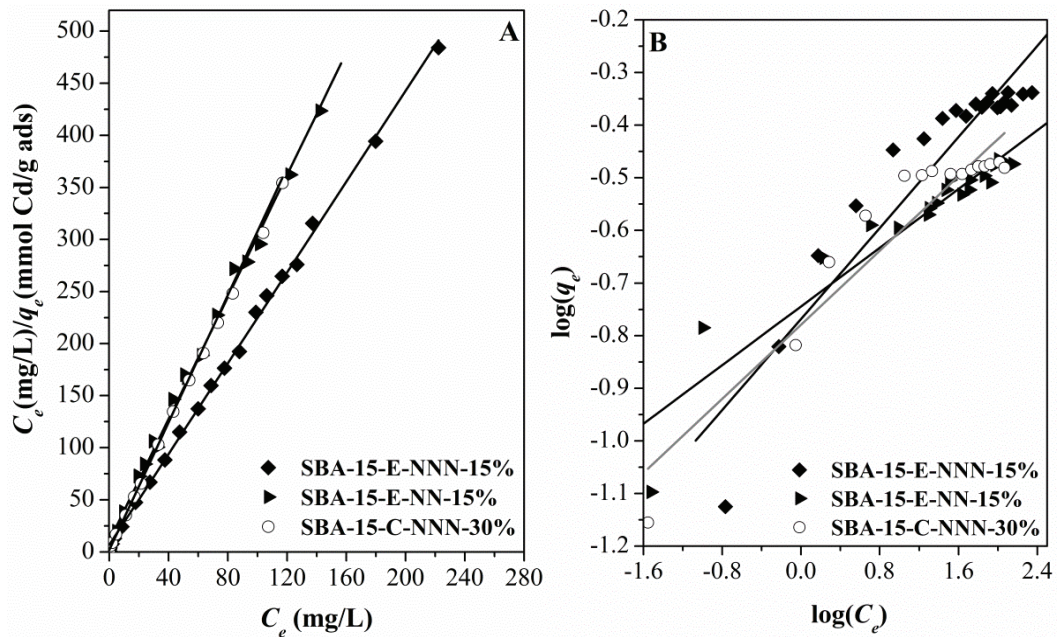


Fig. S5. (A) Linearized Langmuir isotherm plot for adsorption of cadmium(II) on extracted 'E' and calcined 'C' SBA-15 materials functionalized by grafting with NN and NNN organic chains. (B) Linearized Freundlich isotherm plot for adsorption of cadmium(II) on extracted 'E' and calcined 'C' SBA-15 materials functionalized by grafting with NN and NNN organic chains.

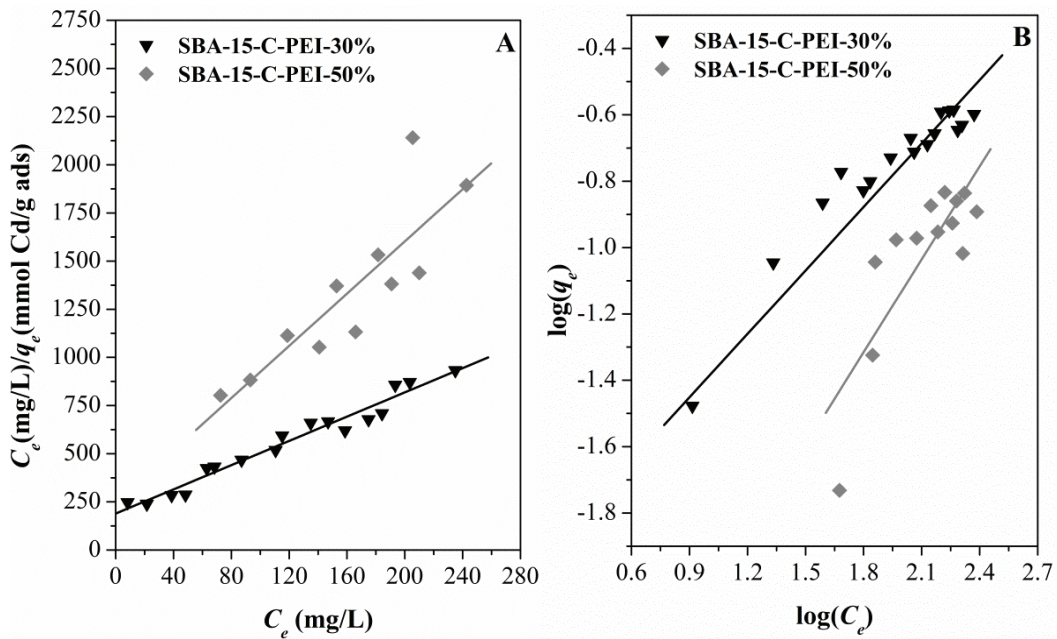


Fig. S6. (A) Linearized Langmuir isotherm plot for adsorption of cadmium(II) on calcined 'C' SBA-15 materials impregnated 30% and 50% with PEI polymer molecules. (B) Linearized Freundlich isotherm plot for adsorption of cadmium(II) on calcined 'C' SBA-15 materials impregnated 30% and 50% with PEI polymer molecules.